Structure of a polytype of the inorganic misfit-layer compound $(PbS)_{1.18}TiS_2$

Sander van Smaalen and Jan L. de Boer
Chemical Physics, Materials Science Center, University of Groningen, Nijenborgh 4, NL 9747 AG Groningen, The Netherlands
(Received 11 March 1992)

A second modification is reported of the inorganic misfit-layer compound $(PbS)_{1.18}TiS_2$. It is found to be a true polytype of the previously analyzed monoclinic form. The *AB* stacking of layers in the latter is replaced by a stacking *AB A'B'* in this orthorhombic modification. Single-crystal x-ray diffraction measurements (Mo $K\alpha$ radiation, $\lambda=0.71073$ Å) were performed on a crystal of $(PbS)_{1.18}TiS_2$. The structure is described by two modulated subsystems ($\nu=1,2$), which have the $(\mathbf{a}_{\nu 2}^*,\mathbf{a}_{\nu 3}^*)$ reciprocal-lattice plane in common. A superspace embedding follows from four reciprocal-lattice vectors, given by $\mathbf{a}_1^*=\mathbf{a}_{11}^*$, $\mathbf{a}_2^*=\mathbf{a}_{12}^*$, $\mathbf{a}_3^*=\mathbf{a}_{13}^*$, and $\mathbf{a}_4^*=\mathbf{a}_{21}^*$. The symmetry is given by the superspace group $G_s=P{:}Cmca(\alpha_0,0,0)\bar{1}ss$. Lattice parameters for the first subsystem (TiS_2) are $a_{11}=3.409(1)$ Å, $a_{12}=5.882(1)$ Å, and $a_{13}=23.409(3)$ Å, with modulation wave vector $\mathbf{q}^1=\mathbf{a}_{21}^*=\alpha_0\mathbf{a}_{11}^*$, and $\alpha_0=0.5875(3)$. Its subsystem superspace group is $P{:}Cmca(\alpha_0,0,0)\bar{1}ss$. The second subsystem (PbS) has lattice parameters $a_{21}=5.802(1)$ Å, $a_{22}=a_{12}$, and $a_{23}=a_{13}$, with modulation wave vector $\mathbf{q}^2=\mathbf{a}_{11}^*$. The subsystem superspace group is $P{:}Cmna(\alpha_0^{-1},0,0)\bar{1}1s$. Refinements on 1123 main reflections and 186 first-order satellites with $I>2.5\sigma(I)$, converged smoothly to $R_{F^2}=0.163$ ($R_F=0.111$). The final structure model included displacive modulation parameters up to second harmonics for Pb, and first harmonics for the other atoms. The largest modulation amplitudes are found on both atoms of the PbS subsystem. They mainly describe displacements parallel to the layers, along the commensurate direction $\mathbf{a}_{\nu 2}$. It is shown that the local structures in the monoclinic and the orthorhombic forms are very much alike.

INTRODUCTION

Inorganic misfit-layer compounds are a special kind of layer compound.[1-4] Their structures are characterized by an alternate stacking of two chemically distinct types of layers. The first type is a three-atom-thick layer of chemical composition TX_2. The second type has composition *MX* and can be characterized as a two-atom-thick (100) slice of a rock-salt-like structure (*X* is S or Se; both *M* and *T* represent a metal atom).

The atoms of the TX_2 layers (first subsystem; $\nu=1$) are ordered with periodicity according to the lattice $\Lambda_1=\{\mathbf{a}_{11},\mathbf{a}_{12},\mathbf{a}_{13}\}$. The atoms of the *MX* layers (second subsystem; $\nu=2$) are ordered with a different periodicity, given by $\Lambda_2=\{\mathbf{a}_{21},\mathbf{a}_{22},\mathbf{a}_{23}\}$. In principle, Λ_1 and Λ_2 are unrelated. However, for all misfit compounds synthesized up to now, it has been found that the $(\mathbf{a}_{\nu 2}^*,\mathbf{a}_{\nu 3}^*)$ reciprocal-lattice plane is common to the subsystems.

The structures of many misfit-layer compounds have been reported. All combinations of stacking sequences have been observed, according to C-centered and F-centered subsystem Bravais lattices. These are combined with either orthorhombic, monoclinic, or triclinic point symmetry. Despite this great variety in structure, each particular compound, as characterized by the elements *T*, *M*, and *X*, has been found in only one space group. True polytypism has not yet been reported.

Recently, we have determined the structure of an inorganic misfit-layer compound with composition $(PbS)_{1.18}TiS_2$.[5] It was found to be monoclinic, with the incommensurate $\mathbf{a}_{\nu 1}$ axes as unique axes [Fig. 1(a)]. The stacking axes $\mathbf{a}_{\nu 3}$ were found to be, from one layer to the next, of the same type. They make a small nonzero angle with the layer normal, which was explained to originate from the specific structure of the TiS_2 layers.[6] In this paper we report on the structure of a crystal with the same chemical composition and taken from the same batch. The stacking axes are perpendicular to the layers, but

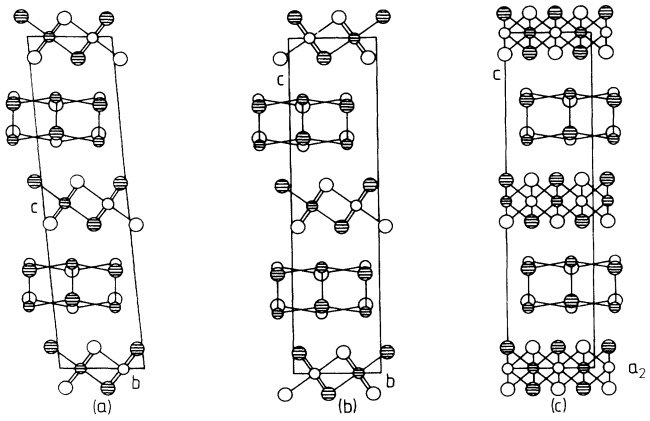

FIG. 1. Projections of the structures of $PbS_{1.18}TiS_2$. Large circles denote sulfur atoms; small circles denote Pb and Ti atoms. Hatched and open circles represent atoms differing 0.5 along the projection axis ($x_{\nu 2}$ or $x_{\nu 1}$). (a) Projection along the $a_{\nu 1}$ axes of the structure of the monoclinic form. Note that two unit cells along $\mathbf{a}_{\nu 3}$ are shown. (b) Similar projection of the structure of the orthorhombic form. (c) Projection of the structure of the orthorhombic form along the $a_{\nu 2}$ axes.

 ©1992 The American Physical Society

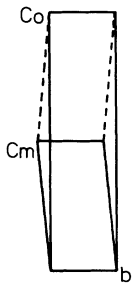

FIG. 2. A monoclinic unit cell put together with its mirror image to produce an orthorhombic unit cell with an almost double-c axis.

they encompass two layers of the each kind. The symmetry of these crystals is found to be orthorhombic.

In a first approximation, the structure of the orthorhombic form of $(PbS)_{1.18}TiS_2$ can be viewed as an alternate stacking of the unit cell of the monoclinic form and a mirror image of this cell (Fig. 2). We will show this picture to be correct, apart from an additional translation parallel to the layers. This makes this new form a true polytype of the previously synthesized monoclinic form.

EXPERIMENT

Three crystals were taken from the same batch as had supplied the monoclinic form of $(PbS)_{1.18}TiS_2$. They were all thicker than the monoclinic crystals. Analysis on an x-ray diffractometer showed that the diffraction pattern of each crystal could be indexed on two mutually incommensurate C-centered orthorhombic unit cells. One crystal, with the approximate dimensions of $0.25\times0.20\times0.01$ mm^3, was selected for data collection.

Single-crystal x-ray diffraction was performed on an Enraf-Nonius CAD-4F diffractometer using monochromatized Mo $K\bar{\alpha}$ radiation ($\lambda=0.71073$ Å). Unit-cell dimensions and their standard deviations were determined for each subsystem independently from the setting angles in four alternate settings of 19 reflections in the range $23.42°<\theta<25.25°$ for TiS_2 and of 21 reflections in the range $24.17°<\theta<25.38°$ for PbS.[7] For TiS_2 (first subsystem; $\nu=1$), lattice parameters were found as $a_{11}=3.4086(3)$ Å, $a_{12}=5.8814(7)$ Å, and $a_{13}=23.406(2)$ Å, with $V_1=469.2(1)$ Å^3. For the PbS subsystem ($\nu=2$), lattice parameters are $a_{21}=5.8020(5)$ Å, $a_{22}=5.8822(8)$ Å, and $a_{23}=23.413(3)$ Å, with $V_2=799.1(2)$ Å^3. The results show that both $a_{\nu2}$ and both $a_{\nu3}$ are equal within standard deviations, indicating a common $(\mathbf{a}^*_{\nu2},\mathbf{a}^*_{\nu3})$ reciprocal-lattice plane, as well as $\mathbf{a}_{12}=\mathbf{a}_{22}$ and $\mathbf{a}_{13}=\mathbf{a}_{23}$. The $\mathbf{a}_{\nu1}$ axes are parallel, but have an incommensurate length ratio $a_{11}/a_{21}=\alpha_0=0.58749(5)$. For the description of the structure the average values of the lattice parameters were used: $a_2=\frac{1}{2}(a_{12}+a_{22})=5.8818(8)$ Å, and $a_3=\frac{1}{2}(a_{13}+a_{23})=23.409(3)$ Å.

From the size of the subsystem unit cells and the number of formula units per cell ($Z=8$ for PbS and $Z=4$ for TiS_2), one finds that the composition of the compound is $(PbS)_xTiS_2$, with $x=1.17497$ for the orthorhombic compound and $x=1.1755$ for the monoclinic compound.[5] Properly rounding off would lead to the seemingly different composition 1.17 and 1.18, respectively. Here we will designate both compounds with $x=1.18$. A more accurate value for the stoichiometry is $x=1.175(1)$.

The data collection was performed separately for the subsystems. Reflection intensities were measured at the nodes of the reciprocal lattices of the respective subsystems, and at the positions of the first-order satellites. All main reflections were measured in one hemisphere up to $\theta=35°$. The experimental stability was checked by the three standard reflections (0,0,8), (0,2,6), and (0,2,−6), measured every 2 h of x-ray exposure time; they showed a long-term variation of less than 2%. The intensities were corrected for the scale variation, Lorentz and polarization effects, and for absorption ($\mu=454.4$ cm^{-1}) using a Gaussian integration method.[8]

For TiS_2, 2257 measured main reflections were combined into 656 unique reflections, using Laue symmetry *mmm*. The internal consistency was $R_I=(\sum|I_i-I_i^{av}|)/(\sum I_i)=0.058$. For PbS, the same Laue symmetry reduced 3795 measured intensities to 1047 unique reflections, with $R_I=0.042$. The common $(0,k,l)$ reflections were used to bring the data sets on the same scale. For 110 reflections present in both data sets, this resulted in a scale factor of 0.9872(7) to multiply the PbS intensities. The internal consistency is found as $R_I=0.010$. The result is a single data set for the misfit compound with 1589 unique main reflections.

First-order satellites were measured up to $\theta_{max}=27°$ in a hemisphere with $k\geq0$. To increase accuracy, reflections with $I\geq2.5\sigma(I)$ were selected for an additional measurement, spending six times more time on each PbS satellite and 24 times more on each TiS_2 satellite. The same corrections were applied as for the main reflections.

The "satellite" data set for TiS_2 comprised 2579 reflections, which were combined into 677 unique reflections using *mmm* symmetry. It contained 91 $|h_1|=0.59$ satellites, which are equal to $|h_2|=1$ main reflections of the PbS subsystem. 115 reflections, with $|h_1|=0.41$ or $|h_1|=4.59$, were overlapping with PbS main reflections. All these reflections were removed. Furthermore, the reduced data set contained 102 $(0,k,l)$ reflections, which were used to bring the TiS_2 satellites onto the same scale as the main reflections. The scale factor was obtained as 1.144(1) with $R_I=0.009$ for 75 common reflections with $I>2.5\sigma(I)$.

Similarly, 4238 satellites of the PbS subsystem were combined into 1086 unique reflections. The latter set contained 87 main reflections of the TiS_2 subsystem and 111 satellites overlapping with TiS_2 main reflections. Again the 102 $(0,k,l)$ reflections present were used to bring these satellites onto the same scale as the main reflections. The scale factor was obtained as 1.142(1) with $R_I=0.009$ for 75 common reflections. It is noted that the reflections with both $|H|=|h_1|=1$ and $|M|=|h_2|=1$ form a plane of common first-order satellites, which were present in both the measured data sets.

Refinements were performed on reflections with $I > 2.5\sigma(I)$. With this criterion for observability, the number of unique reflections reduced to 1309 [108$(0,k,l)$ reflections, 353 main reflections of the TiS_2 subsystem, 663 for PbS, and 186 satellites].

SUPERSPACE-GROUP SYMMETRY

The starting point of the superspace-group approach is the description of the diffraction pattern with a finite set of integer indices.[9-12] The common $(\mathbf{b}^*,\mathbf{c}^*)$ plane implies that four reciprocal vectors are sufficient to obtain an integer indexing of the complete diffraction pattern. This set, $M=\{\mathbf{a}_1^*,\mathbf{a}_2^*,\mathbf{a}_3^*,\mathbf{a}_4^*\}$, can be defined as $\mathbf{a}_1^*=\mathbf{a}_{11}^*$, $\mathbf{a}_2^*=\mathbf{a}_{12}^*$, $\mathbf{a}_3^*=\mathbf{a}_{13}^*$, and $\mathbf{a}_4^*=\mathbf{a}_{21}^*$. The $\mathbf{a}_{vi}^*$ $(v=1,2;i=1,2,3)$ are the reciprocal-lattice vectors of the subsystem unit cells as defined in the experimental section. Superspace is obtained in the usual way, by identification of the four basis vectors of M with the perpendicular projection of four independent translation vectors in a $(3+1)$-dimensional space.[9,13] The fourth element of M can be expressed in the first three. This defines the incommensurability, expressed by the σ matrix:

$$\sigma=(\alpha_0,0,0) \ . \tag{1}$$

The basis vectors of the subsystem reciprocal lattices Λ_v^*, together with the subsystem modulation wave vectors $\mathbf{q}^v$, can be written as an integral linear combination of the basis vectors in M:[10,11]

$$\mathbf{a}_{vi}^*=\sum_{k=1}^{4} W_{ik}^v \mathbf{a}_k^* \ , \quad i=1,2,3 \ , \tag{2}$$

$$\mathbf{q}^v=\sum_{k=1}^{4} W_{4k}^v \mathbf{a}_k^* \ . \tag{3}$$

That both the basic structure periodicities Λ_v and the modulation wave vectors are derived from the same set of reciprocal vectors M expresses the fact that each subsystem is modulated with a modulation wave vector given by the periodicities of the reciprocal lattice of the other subsystem.

For the present analysis the following matrices will be used:

$$W^1=\begin{bmatrix} 1 & 0 & 0 & 0 \\ 0 & 1 & 0 & 0 \\ 0 & 0 & 1 & 0 \\ 0 & 0 & 0 & 1 \end{bmatrix} , \quad W^2=\begin{bmatrix} 0 & 0 & 0 & 1 \\ 0 & 1 & 0 & 0 \\ 0 & 0 & 1 & 0 \\ 1 & 0 & 0 & 0 \end{bmatrix} . \tag{4}$$

The W^v matrices can be interpreted as defining a coordinate transformation in superspace, between the superspace axes corresponding to M and the standard superspace for each subsystem. For example, W^v gives the relation between the subsystem indexing of reflections and the indexing on M [Eqs. (2) and (3)]:

$$(H,K,L,M)=(h_v,k_v,l_v,m_v)W^v \ . \tag{5}$$

Considering the superspace indexing, the diffraction pattern again has orthorhombic symmetry, now generated by $(m_x\bar{1})$, $(m_y 1)$, and $(m_z 1)$. Systematic extinctions are found to be $H+K+M=$odd is absent for the (H,K,L,M) reflections. This implies a C centering given by the centering translation

$$(\tfrac{1}{2},\tfrac{1}{2},0,\tfrac{1}{2}) \ . \tag{6}$$

The $(3+1)$-dimensional Bravais class follows as $P{:}Cmmm(\alpha_0,0,0)\bar{1}11$,[13] with C a tentative symbol representing the centering translation Eq. (6).

Other extinction conditions are found for special subsets of reflections: $L=2n$, is present for the $(00L0)$ reflections; $L+M=2n$ and $H+L=2n$ for the $(H0LM)$ reflections; $H+M=2n$ and $K=2n$ for the $(HK0M)$ reflections,; and $H=2n$ and $M=2n$ for the $(H00M)$ reflections (n is an integer). The superspace group explaining all these extinctions is $G_s=P{:}Cmca(\alpha_0,0,0)\bar{1}ss$. It is noted that the extinction condition corresponding to the c glide is violated by some weak reflections among the main reflections and satellites of the PbS subsystem, whereas the a glide and b glide are violated among the TiS_2 main reflections. Refinements showed that subgroups of G_s cannot explain these additional reflections. Therefore, we conclude that G_s is the group describing the symmetry of orthorhombic $(PbS)_{1.18}TiS_2$.

With the coordinate transformation defined by the matrices W^v [Eq. (4)], the elements $(R_s^v|\tau_s^v)$ of the subsystem superspace groups can be defined as[10,11]

$$R_s^v=W^v R_s (W^v)^{-1} \ , \tag{7a}$$

$$\tau_s^v=W^v\tau_s \ . \tag{7b}$$

For the subsystem superspace groups one thus obtains, $G_s^1=G_s$ and $G_s^2=P{:}Cmna(\alpha_0^{-1},0,0)\bar{1}1s$ with, again, C defined by Eq. (6). Note that G_s^1 and G_s^2 are equivalent. The different notation reflects the fact that both subsystem-space groups are described with respect to a different origin. The elements of $G_s=G_s^1$ and of G_s^2 are given in Table I. Similarly, the space groups describing the symmetry of the basic structure of each subsystem can be obtained as the restriction of G_s^v to three-dimensional space. One obtains $G_1=Cmca$ and

TABLE I. Elements of the superspace group G_s, together with the corresponding elements of both subsystem superspace groups G_s^v, $v=1,2$. The listed element may be combined with any of the lattice translations or with the centering translation, n_i, $i=1,2,3,4$ assumes all integer values.

$G_s=G_s^1$	G_s^2
$(E1\|n_1,n_2,n_3,n_4)$	$(E1\|n_4,n_2,n_3,n_1)$
$(E1\|\frac{1}{2},\frac{1}{2},0,\frac{1}{2})$	$(E1\|\frac{1}{2},\frac{1}{2},0,\frac{1}{2})$
$(2_x1\|0,0,0,\frac{1}{2})$	$(2_x1\|\frac{1}{2},0,0,0)$
$(2_y\bar{1}\|\frac{1}{2},0,\frac{1}{2},0)$	$(2_y\bar{1}\|0,0,\frac{1}{2},\frac{1}{2})$
$(2_z\bar{1}\|\frac{1}{2},0,\frac{1}{2},\frac{1}{2})$	$(2_z\bar{1}\|\frac{1}{2},0,\frac{1}{2},\frac{1}{2})$
$(i\bar{1}\|0,0,0,0)$	$(i\bar{1}\|0,0,0,0)$
$(m_x\bar{1}\|0,0,0,\frac{1}{2})$	$(m_x\bar{1}\|\frac{1}{2},0,0,0)$
$(m_y1\|\frac{1}{2},0,\frac{1}{2},0)$	$(m_y1\|0,0,\frac{1}{2},\frac{1}{2})$
$(m_z1\|\frac{1}{2},0,\frac{1}{2},\frac{1}{2})$	$(m_z1\|\frac{1}{2},0,\frac{1}{2},\frac{1}{2})$

$G_2 = Cmna$. Again both subsystem-space groups are equivalent.

THE STRUCTURE

Each section in superspace perpendicular to the additional dimension gives an equivalent description for physical space. It is characterized by the parameter t.[5,12,14] With respect to the subsystem lattice Λ_ν, the coordinates of atom j of subsystem ν in such a section t can be written as

$$x_{\nu i}(j) = \bar{x}_{\nu i}(j) + u^j_{\nu i}(\bar{x}_{\nu s4}) \tag{8}$$

for $\nu = 1,2$ and $i = 1,2,3$. From Eqs. (1)–(4) the basic structure coordinates $\bar{x}_{\nu i}$ follow as[5]

$$\begin{aligned} \bar{x}_{1i}(j) &= n_{1i} + x^0_{1i}(j) \ , \quad i = 1,2,3 \ , \\ \bar{x}_{21}(j) &= n_{21} + x^0_{21}(j) - t \ , \\ \bar{x}_{2i}(j) &= n_{2i} + x^0_{2i}(j) \ , \quad i = 2,3 \ , \end{aligned} \tag{9}$$

where $n_{\nu i}$ runs over all integers, and $x^0_{\nu i}(j)$ are the coordinates of atom j with respect to the subsystem unit cell. These are the ones determined in the structure refinement. The modulation functions $u^j_{\nu i}(\bar{x}_{\nu s4})$ are periodic, with periodicity one. Their arguments are the fourth superspace coordinates of the subsystems[5]

$$\begin{aligned} \bar{x}_{1s4} &= \alpha_0 \bar{x}_{11}(j) + t \ , \\ \bar{x}_{2s4} &= \alpha_0^{-1}[\bar{x}_{21}(j) - t] \ . \end{aligned} \tag{10}$$

Evidence that the orthorhombic compound is a polytype of monoclinic form was provided by comparing the unit-cell dimensions. With α unequal to 90°,[5] an orthorhombic lattice can be constructed from the monoclinic one by having the c axis pointing alternately left and right (Fig. 2). The resulting orthorhombic c axis has length $c(0) = 2\sin(\alpha)c(m) = 23.419$ Å. This compares very well with the experimentally determined value of $a_{23} = 23.409(3)$ Å. Note that $2c(m) = 23.518(4)$ Å.

Assuming the orthorhombic compound to be such a polytype, the coordinates of the atoms in the lower half of the unit cell were obtained from the monoclinic structure by referring the latter coordinates with respect to the orthorhombic cell. With the proper choice of origin, all atoms in the orthorhombic unit cell were generated by the symmetry elements (Table I). Refinements of the basic structure coordinates showed the initial guess to be correct, since a reasonable fit was obtained (Table II). The final coordinates did differ only marginally from those derived from the monoclinic structure (Fig. 1). All refinements were performed with the computer program COMPREF from the program system JANA.[15,16]

The complete structure also involves modulation functions for each atom. In the basic structure Ti is on an inversion center $i = 2_x/m_x$, while the other atoms are in the mirror m_x. The corresponding superspace operators lead to restrictions on the modulation functions (Table III).

The modulation functions can be written as a Fourier series:

$$u^j_{\nu i}(\bar{x}_{\nu s4}) = \sum_{n=1}^{\infty} A^j_{ni}\sin(2\pi n \bar{x}_{\nu s4}) + B^j_{ni}\cos(2\pi n \bar{x}_{\nu s4}) \ . \tag{11}$$

It appeared that for each atom the first harmonic ($n = 1$) could be refined, while for Pb the second harmonic was also included in the refinement. More harmonics led to a singular matrix. Only those parameters were employed that are compatible with the superspace-group symmetry (Table III). The main effect of the modulation was to reduce the partial R factor for the TiS_2 main reflections, while a reasonable fit of all first-order satellites was obtained (Table II). The refinements also included anisotropic temperature factors, a scale factor, and an isotropic parameter describing secondary extinction. The results of the refinement of the modulated structure are summarized in Tables IV and V.

The R factors for the best model are still rather high (Table II). In the search for other solutions, structure models were tried in lower symmetries, ranging from acentric orthorhombic to monoclinic. Refinement of the additional parameters introduced in this way did not lead to a significant lowering of the R factors, while the structure remained essentially the same as described in G_s. It was therefore concluded that the relatively large $\Delta F = (F_{\rm obs} - F_{\rm calc})$ values must have another origin.

TABLE II. Reliability factors for the final fits, with and without the modulation, respectively. The R factors are defined as $R_F = (\sum \| F_{\rm obs}| - |F_{\rm calc}\|)/\sum |F_{\rm obs}|$ and $R_{F^2} = [\sum (|F_{\rm obs}| - |F_{\rm calc}|)^2 / \sum |F_{\rm obs}|^2]^{1/2}$. Partial R factors are defined using a subset of the reflections. The TiS_2 part and PbS part comprise the main reflections of the corresponding subsystem, excluding the common reflections $(0,K,L,0)$.

Reflection subset	Number of reflections	Basic structure R_F	Basic structure R_{F^2}	Modulated structure R_F	Modulated structure R_{F^2}
All	1309	0.115	0.144	0.111	0.163
First-order satellites	186			0.161	0.168
TiS_2 part	353	0.152	0.180	0.122	0.172
PbS part	663	0.111	0.135	0.112	0.167
Common	108	0.082	0.116	0.085	0.122

TABLE III. Symmetry restrictions on the modulation functions. The restrictions apply to the modulation functions as defined in Eqs. (8)–(11), with symmetry operators from Table I. For each atom it is given whether the function is odd, even, or zero.

	Coordinate	Odd harmonics	Even harmonics
Ti ($\nu=1$)	u_{11}	zero	odd
	u_{12}	odd	zero
	u_{13}	odd	zero
S1 ($\nu=1$)	u_{11}	even	odd
	u_{12}	odd	even
	u_{13}	odd	even
Pb ($\nu=2$)	u_{21}	odd	odd
	u_{22}	even	even
	u_{23}	even	even
S2 ($\nu=2$)	u_{21}	odd	odd
	u_{22}	even	even
	u_{23}	even	even

One factor influencing the quality of the fit is stacking faults. Their precise nature is difficult to determine, and certainly cannot be described by a lowering of the symmetry. Two types of such faults can be distinguished. The first can be described as having consecutive layers that assume the monoclinic-type stacking instead of the normal alternating left-right stacking (Fig. 3). Since no reflections corresponding to the monoclinic cell could be observed, this kind of fault is probably not too important.

The second type of stacking faults is related to the structure within each subsystem. Two nearest layers of the same kind may be on top of each other, or may be shifted over $\frac{1}{2}\mathbf{a}_{\nu 1}$. Allowing these two possible stackings for both subsystems gives four possible structures (see next section). The incidental occurrence of other types of stacking can also explain the presence of certain reflections, which would be absent in a fault-free sample with symmetry G_s.

Another important phenomenon, inherent in incommensurate crystals, is that reflections can be found that are arbitrarily close to each other. For reflections with a finite width ($\Delta\lambda$ effect, mosaic spread) this implies that some reflections are measured at the same position. Usually, this overlap is between strong reflections and satellites of much higher order, the latter with virtual zero intensity. Unique to the intergrowth compounds is that such an overlap also occurs between main reflections of the respective subsystems, and between main reflections of one subsystem with low-order satellites of the other subsystem.[3] For $(PbS)_{1.18}TiS_2$, the special value of $\alpha_0=0.587\simeq 0.6=\frac{3}{5}$ determines a partial overlap between the $h_1=3$, $(3,K,L,0)$ main reflections of TiS_2 and the $h_2=5$, $(0,K,L,5)$ main reflections of PbS. Inspection of the reflection list shows the largest $|\Delta F|$ values to be among these two subsets. It was already noted in the ex-

TABLE IV. Basic structure coordinates and temperature parameters (Å^2) as obtained by refinement of the modulated structure. Coordinates refer to the subsystem lattices. Standard deviations in the last digits are in parentheses. The temperature factor that appears in the expression for the structure factor is defined by

$$T=\exp\left[-2\pi^2\sum_{i,j=1}^{3}U_{ij}a^*_{\nu i}a^*_{\nu j}h_{\nu i}h_{\nu j}\right].$$

U_{12} and U_{13} are zero as a consequence of the symmetry.

	ν	$x^0_{\nu 1}$	$x^0_{\nu 2}$	$x^0_{\nu 3}$	
Ti	1	0.0	0	0	
S1	1	0.0	0.3353(5)	0.0611(2)	
Pb	2	0.75	0.0944(2)	0.31823(6)	
S2	2	0.25	0.0954(12)	0.2994(4)	
		U_{11}	U_{22}	U_{33}	U_{12}
Ti	1	0.010(1)	0.004(1)	0.017(2)	−0.000(1)
S1	1	0.010(1)	0.003(1)	0.013(1)	−0.000(1)
Pb	2	0.0396(7)	0.0252(6)	0.0254(7)	−0.0005(5)
S2	2	0.045(4)	0.018(3)	0.031(4)	−0.002(3)

TABLE V. Modulation parameters. Values are given for $A^j_{ni}a_{\nu i}$ and $B^j_{ni}a_{\nu i}$ (Å). For $j=$Ti, S1 ($\nu=1$), the values correspond to $B_{n1}a_{11}$, $A_{n2}a_{12}$, and $A_{n3}a_{13}$. For $j=$Pb, S2 ($\nu=2$), the values correspond to $A_{n1}a_{21}$, $B_{n2}a_{22}$, and $B_{n3}a_{23}$ [Eq. (11) and Table III]. Standard deviations in the last digits are in parentheses.

	A^j_{n1}/B^j_{n1}	A^j_{n2}/B^j_{n2}	A^j_{n3}/B^j_{n3}
	First harmonic ($n=1$)		
Ti	0.0	0.004(4)	−0.014(7)
S1	−0.008(10)	0.001(4)	−0.017(7)
Pb	0.001(3)	0.059(1)	0.025(3)
S2	−0.01(2)	−0.046(7)	0.03(2)
	Second harmonic ($n=2$)		
Pb	0.021(3)	0.004(5)	0.003(5)

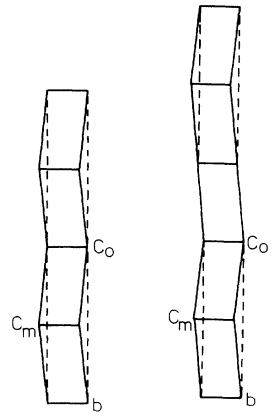

FIG. 3. Arrangement of the monoclinic subcells comprising the orthorhombic unit cell, in the normal structure (left), and with a monoclinic stacking fault (right).

periment section that some reciprocal layers of satellites had to be removed due to a partial overlap with the main reflections. At the same time, the corresponding main reflections will have been contaminated by the satellites. These reflections will also be fitted less well than is to be expected for a conventional structure.

The considerations presented above lead us to conclude that the model presented here correctly describes the ideal, fault-free structure of the orthorhombic form of $(PbS)_{1.18}TiS_2$.

DISCUSSION

In each subsystem there is only one crystallographically independent atom of each type (Table IV). From Fig. 1 it then follows that there is only one type of atomic plane in the PbS subsystem, and only one type of sulfur plane in the TiS_2 subsystem. Consequently, there is also only one type of plane of contact between the two subsystems. As for the other misfit-layer compounds, the shortest distances between the two subsystems are between the sulfur atoms of the first subsystem and lead atoms of the other subsystem.

To study the intersubsystem bonding, it was proposed to plot the interatomic distances as a function of the fourth superspace parameter t.[5,12,14] The distance between one atom of the second subsystem at $\bar{x}_2$(Pb), and one atom of the first subsystem at $\bar{x}_1$ (S1) becomes infinite for $t \rightarrow \pm\infty$ [Eq. (9)], as is illustrated by one of the paraboliclike curves in Fig. 4. However, the distances from a single Pb to all sulfur atoms of the first subsystem together form a plot periodic in t, with the same periodicity as for the second subsystem itself, i.e., with periodicity $\alpha_0=0.59$ (Fig. 4).[5,12]

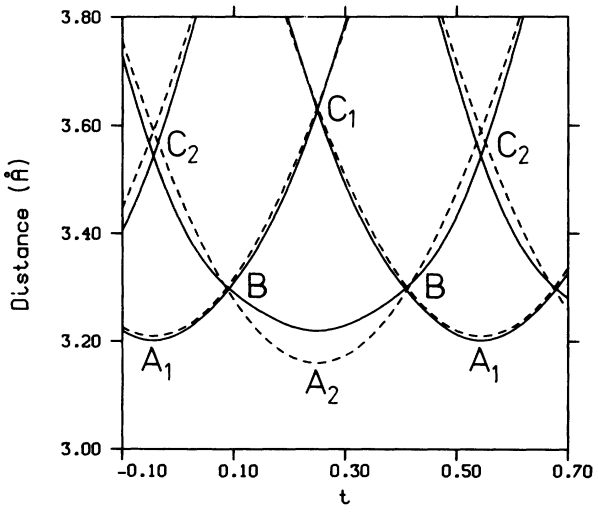

FIG. 4. Coordination of Pb ($\nu=2$) by S1 ($\nu=1$) as a function of the fourth superspace coordinate t. Distances are given for the basic structure (broken curves) and for the modulated structure (full lines). The curves are from Pb at $(0.25,x^0_{22},0.5-x^0_{23},0.5+\bar{x}_{2s4})$ to S1 at $(0.5+n_{11}, -0.5+x^0_{22},x^0_{23},0.5+\bar{x}_{1s4})$ for the curves marked A_1 and to S1 at $(n_{11},x^0_{22},x^0_{23},\bar{x}_{1s4})$ for the curves marked A_2 (n_{11} is integer; x^0_{vi} from Table IV). Equally marked curves correspond to different values for n_{11}, i.e., to different but translationally equivalent sulfur atoms.

The interpretation of Fig. 4 is that all distances read off at a single value of t represent the coordination of Pb by S1 somewhere in the crystal. All existing coordinations are represented in one period along the t axis. The effect of the modulation is to increase the Pb to S1 distance at points where they are closest (A_2 in Fig. 4). Furthermore, the variation in the shortest distance decreases from 0.14 Å in the basic structure to 0.09 Å in the real structure. It appears that this variation is of the same order as the variation in the individual Pb to S2 distances within the periodic second subsystem (0.06 Å), and it is much smaller than the range of Pb to S2 distances (0.23 Å). The effect of the incommensurateness in the basic structure on the first coordination shell is surprisingly small, which probably is an important feature determining the stability of the misfit-layer compounds.[14] Comparing the distances between Pb and S1 with the corresponding distances in the monoclinic form shows that the plane of contact is to a large extent similar in both polytypes (Figs. 4 and 5; Table VI).

The structure of the individual layers is almost the same in the orthorhombic and the monoclinic form. Comparing the modulation functions shows that in both compounds the main displacements are on the atoms of the PbS subsystem, along the commensurate in-plane direction $\mathbf{a}_{\nu 2}$. For the orthorhombic form, the component along **c** of the Pb modulation also has a relatively large amplitude. Unfortunately, in the present refinement the standard deviations for the modulation parameters of the other atoms, especially of S2, are rather large.

The structure of the individual layers is centered rectangular. This implies a C centering in the lattice of the

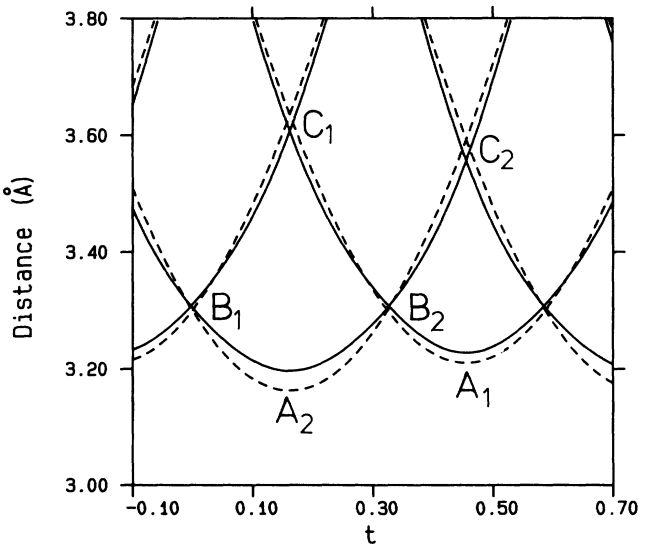

FIG. 5. Coordination of Pb ($\nu=2$) by S1 ($\nu=1$) for the monoclinic form as a function for the fourth superspace coordinate t (after Ref. 5). Distances are given for the basic structure (broken curves) and for the modulated structure (full lines).

TABLE VI. Selected interatomic distances compared to the corresponding distances in the monoclinic form.[5] Distances are given between Pb and S1 (see Figs. 4 and 5) and between Pb and the five closest symmetry equivalents of S2.

	Basic structure		Modulated structure	
Atom pair	orthorhombic form [Å]	monoclinic form [Å]	orthorhombic form [å]	monoclinic form [Å]
A_1	3.21	3.21	3.20	3.23
A_2	3.16	3.16	3.21	3.20
B	3.29	3.30	3.29	3.31
C_1	3.62	3.64	3.61	3.61
C_2	3.58	3.59	3.53	3.56
S2 along **c**	2.755	2.755		
S2 at $\pm\frac{1}{2}\mathbf{a}_{21}$	2.935	2.933		
S2 at $-\frac{1}{2}\mathbf{a}_{22}$	2.967	2.971		
S2 at $\frac{1}{2}\mathbf{a}_{22}$	2.980	2.975		

complete crystal. For the simple misfit-layer compounds, with an AB sequence of the layers, two consecutive layers of the same kind (e.g., A) can be right on top of each other, or they can have an additional shift of $\frac{1}{2}\mathbf{a}_{\nu 2}$. Combined with the C centering, the latter implies a F-centered lattice for subsystem ν. This notation led to a classification of the simple misfit-layer compounds in four types, as characterized by the combinations of stackings in the respective subsystems: CC, CF, FC, and FF.[2,3]

For the monoclinic form the **c** axes have been defined to make the smallest possible angle with the normal to the planes [5.27(2)°].[5] The stacking of the layers in the monoclinic form could then be identified as CC type with, for both subsystems, $c=11.76$ Å.[5] Comparing the structures of the orthorhombic form and the monoclinic form shows that the PbS subsystem in o-$(PbS)_{1.18}TiS_2$ has again a C-type stacking, with a pseudotranslation vector equal to the **c** axis in the monoclinic form (Fig. 1). Alternately, this axis turns 5.27° to the left and to the right, thus resulting in the orthorhombic structure with an approximate doubled **c** axis.

For the sulfur planes of the TiS_2 subsystem of the orthorhombic form, a C-type stacking with a pseudotranslation vector equal to the **c** axis of the monoclinic form, is also found. However, when the top planes of two consecutive layers have a pseudotranslation vector tilting 5.27° to the left, the bottom planes have the pseudotranslation vector tilting to the right. This is a result of the fact that in order to derive the structure of the orthorhombic form from the structure of the monoclinic form, not only every other TiS_2 layer is replaced by its m_z mirror image but, in addition, it is translated over $(\frac{1}{2},\frac{1}{6},0)$. This same translation then determines that the Ti atoms assume a F-type stacking, with the pseudotranslation vector now perpendicular to the layers.

Extending the former classification of stacking types,[2,3] orthorhombic $(PbS)_{1.18}TiS_2$ can be characterized as of the C(F)C type. The C symbols refer to the stacking of the sulfur planes of TiS_2 and of the PbS subsystem, respectively, while the F symbol gives the stacking type of Ti as is implied by the structure of the sulfur planes. The other types of stacking also have their counterpart among the double-**c**-axis orthorhombic structures, i.e., F(C)C, C(F)F, and F(C)F. The corresponding superspace groups are $P{:}Cmcm(\alpha_0,0,0)\bar{1}1s$, $P{:}Cmca(\alpha_0,0,0)\bar{1}1s$, and $P{:}Cmcm(\alpha_0,0,0)\bar{1}ss$. Note that the different stackings now correspond to different translation components combined with rotational operators, and not to different centering translations as for the simple misfit layer compounds.

As noted in the preceding section, the occurrence of the stackings other than C(F)C, may be an important source of the stacking faults. From the superspace-group symbols, it follows that the extinction conditions are different for the alternative symmetries, and that the observed violation of the extinction conditions corresponding to G_s can be explained by parts of the crystal having one of the other symmetries.

CONCLUSIONS

Detailed structural information is given for the inorganic misfit-layer compound $(PbS)_{1.18}TiS_2$. It is shown that this form, with orthorhombic symmetry, is a polytype of the previously reported monoclinic structure of $(PbS)_{1.18}TiS_2$.[5] The stacking AB in the latter compound is replaced by a stacking $ABA'B'$ in the orthorhombic form. Layers A and A', as well as layers B and B', have identical structures as a result of the superspace group symmetry.

The structures of the corresponding, individual layers appeared to be the same in both polytypes. The orthorhombic superspace group determines that in the orthorhombic form there is only one type of plane of interaction between the subsystems. This interaction can be characterized by its shortest interatomic distances, which are between Pb and S of the TiS_2 subsystem. The local structure around these atoms was shown to be the same in the two polytypes, both for the basic structure arrangement and for the modulation functions.

ACKNOWLEDGMENT

The research of one of us (S.v.S.) has been made possible by financial support from the Royal Netherlands Academy of Arts and Sciences (KNAW).

[1]E. Makovicky and B. G. Hyde, Struct. Bonding (Berlin) **46**, 101 (1981).

[2]G. A. Wiegers, A. Meetsma, S. van Smaalen, R. J. Haange, J. Wulff, T. Zeinstra, J. L. de Boer, S. Kuypers, G. Van Tendeloo, J. Van Landuyt, S. Amelinckx, A. Meerschaut, P. Rabu, and J. Rouxel, Solid State Commun. **70**, 409 (1989).

[3]S. van Smaalen, in *Incommensurate Sandwiched Layered Compounds,* edited by A. Meerschaut (Trans Tech, Aedermannsdorf, Switzerland, 1992).

[4]G. A. Wiegers and A. Meerschaut, in *Incommensurate Sandwiched Layered Compounds* (Ref. 3).

[5]S. van Smaalen, A. Meetsma, G. A. Wiegers, and J. L. de Boer, Acta Crystallogr. Sect. B **47**, 314 (1991).

[6]G. A. Wiegers, A. Meetsma, S. van Smaalen, R. J. Haange, and J. L. de Boer, Solid State Commun. **75**, 689 (1990).

[7]J. L. de Boer and J. M. Duisenberg, Acta Crystallogr. Sect. A **40**, C-410 (1984).

[8]A. L. Spek, in *Computational Crystallography,* edited by D. Sayre (Clarendon, Oxford, 1982), p. 528.

[9]A. Janner and T. Janssen, Acta Crystallogr. Sect. A **36**, 408 (1980).

[10]S. van Smaalen, J. Phys. Condens. Matter **1**, 2791 (1989).

[11]S. van Smaalen, Phys. Rev. B **43**, 11 330 (1991).

[12]S. van Smaalen, in *Methods of Structural Analysis of Modulated Structures and Quasicrystals,* edited by J. M. Perez-Mato, F. J. Zuniga, and G. Madariaga (World Scientific, Singapore, 1991), pp. 90–106.

[13]P. M. de Wolff, T. Janssen, and A. Janner, Acta Crystallogr. Sect. A **37**, 625 (1981).

[14]S. van Smaalen, J. Phys. Condens. Matter **3**, 1247 (1991).

[15]V. Petricek, K. Maly, P. Coppens, X. Bu, I. Cisarova, and A. Frost-Jensen, Acta Crystallogr. A **47**, 210 (1991).

[16]V. Petricek, K. Maly, and I. Cisarova, in *Methods of Structural Analysis of Modulated Structures and Quasicrystals* (Ref. 12), pp. 262–267.